applied sciences

MDPI

Review

Nanomaterials-Enabled Electrochemical Biosensors: From Enhanced Performance to Regulatory Readiness

Virginia Rondinini [1], Stefano Giordani [1,2,3,*], Luisa Stella Dolci [3,4], Anna Placci [1,2,3], Pierluigi Reschiglian [1,2,3], Barbara Roda [1,2,3], Aldo Roda [1,3], Valentina Marassi [1,2,3,*] and Andrea Zattoni [1,2,3]

1 Department of Chemistry "Giacomo Ciamician", University of Bologna, 40129 Bologna, Italy
2 byFlow srl, 40129 Bologna, Italy
3 INBB—Biostructures and Biosystems National Institute, 00165 Rome, Italy
4 Department of Industrial Chemistry "Toso Montanari", University of Bologna, 40129 Bologna, Italy
* Correspondence: stefano.giordani7@unibo.it (S.G.); valentina.marassi@unibo.it (V.M.)

Abstract

Electrochemical biosensors represent mature platforms for point-of-need analysis due to their high sensitivity, intrinsic selectivity, low cost, and facile miniaturization. In the last decade, nanomaterials have become integral to advanced biosensor architectures, acting as high-surface-area supports, electron-transfer mediators, and signal-amplifying elements. This review critically examines the most represented nanomaterial classes in mature electrochemical biosensors—carbon nanostructures, gold nanoparticles, and iron-based magnetic nanoparticles—highlighting how morphology, electronic structure, and surface chemistry influence key performance metrics such as limit of detection, linear range, and assay time. Despite a strong technology push and numerous proof-of-concept demonstrations, the translation of nanomaterial-enabled electrochemical biosensors into commercial devices remains limited. This gap arises from the intrinsic physicochemical complexity of nanomaterials, which hampers standardization, reproducibility, and long-term safety assessment. Accordingly, this review integrates performance analysis with a systematic overview of the European regulatory framework, including the Medical Device Regulation (MDR) (EU) 2017/745, the In Vitro Diagnostic Regulation (IVR) (EU) 2017/746, EFSA guidance for food and water applications, and relevant ISO standards, outlining key translational bottlenecks and design principles for deployable biosensing technologies.

Keywords: electrochemical biosensors; nanomaterials; carbon nanostructures and nanotubes (CNTs); graphene nanostructures; gold nanoparticles; magnetic nanoparticles; regulatory framework; clinical market; guidelines

Academic Editor: Junseop Lee

Received: 22 December 2025
Revised: 9 February 2026
Accepted: 10 February 2026
Published: 19 February 2026

1. Introduction

Biosensors are analytical devices that couple a biological recognition element (enzymes, antibodies, nucleic acids, cells, or engineered receptors) with a physico-chemical transducer that converts recognition events into measurable signals [1]. The field of biosensors has grown through the convergence of chemistry, biology, electronics, materials science, and engineering. Electrochemical biosensors are the most widely developed and applied class [2]. These systems integrate biorecognition layers with electrochemical transducers to generate quantitative or semi-quantitative outputs—such as current, potential, or impedance—arising from redox reactions or local ionic changes at the electrode interface. Since the seminal glucose enzyme electrode reported by Clark and Lyons in

1962, electrochemical biosensors have become central to diagnostics, environmental monitoring, and industrial process control, owing to their high sensitivity, low cost, ease of miniaturization, and compatibility with scalable manufacturing [3,4]. Their applications span biomedicine, food systems, and environmental analysis, encompassing metabolites, biomarkers, pathogens, contaminants, and pollutants (Figure 1).

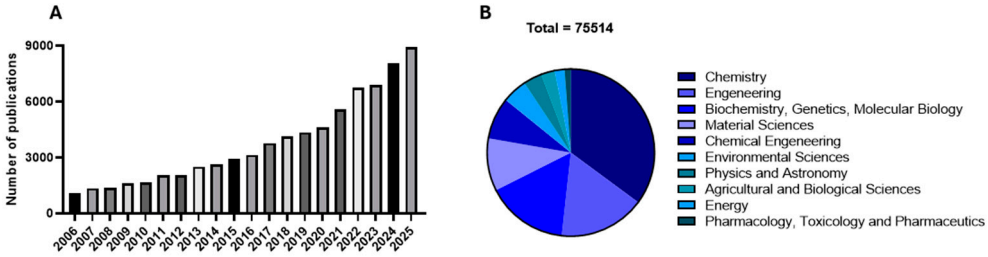

Figure 1. Data retrieved from Scopus using the keywords "Electrochemical biosensors". (**A**) Annual publication count (covering the years 2006 through 2025); (**B**) Distribution across various research fields where these publications appear.

However, conventional electrochemical biosensors based on planar metal or carbon electrodes are intrinsically constrained by surface-governed phenomena, including limited electroactive area, restricted biomolecule loading density, suboptimal interfacial electron-transfer kinetics, and poor scalability toward miniaturized and integrated device formats. As extensively discussed in the literature [5,6], overcoming these limitations cannot be achieved through surface chemistry alone, but progressively requires the co-integration of advanced electrode materials, engineered device architectures, and nanostructured components. In this context, nanomaterials have become integral elements of state-of-the-art electrochemical biosensors due to their high surface-to-volume ratios, tunable electronic properties, and ability to modulate interfacial processes [7]. They are employed both as functional electrode modifiers—enhancing charge-transfer efficiency and mass transport—and as signal-amplifying labels capable of carrying multiple reporter units, enabling sensitivities comparable to or exceeding those of conventional enzyme-based systems [8–12]. A key advance is the strategic integration of nanomaterials at the electrode–solution interface, where electron-transfer kinetics and biomolecular recognition are jointly governed. Metal nanoparticles, carbon nanotubes, and graphene-based networks introduced at this interface increase the effective electroactive surface area, enable controlled biomolecule immobilization, and shorten electron-transfer pathways, thereby improving sensitivity and selectivity [13]. Importantly, the integration of diverse electrode materials and nanostructures is not merely a matter of technological diversification or performance enhancement, but a need dictated by the heterogeneity of analytical targets [14]. Different analytes—ranging from small molecules to nucleic acids and whole cells—impose distinct requirements in terms of surface chemistry, operating potential windows, and immobilization strategies that cannot be universally addressed by a single material platform. For instance, enzymatic glucose sensors typically exploit carbon-based electrodes with wide potential windows and low background currents, whereas DNA hybridization assays preferentially rely on gold electrodes to enable thiol-based self-assembled monolayers and controlled probe orientation [5].

While these strategies enabled numerous proof-of-concept demonstrations, they have not translated proportionally into market-ready devices. The physicochemical complexity of nanomaterials—including batch-to-batch variability, surface heterogeneity, and size-dependent properties—poses significant challenges for standardization, reproducibility, and long-term safety assessment, thereby delaying translation and increasing regulatory scrutiny related to quality control, environmental impact and safety. Consequently, the

limited commercial uptake of nanomaterial-enabled electrochemical biosensors cannot be ascribed solely to technical performance, but must be understood within a broader regulatory context. In particular, the lack of harmonized international guidelines for nanomaterial safety evaluation, together with growing public and regulatory concern regarding nanotoxicity, represent a critical bottleneck for translation.

This review addresses this critical gap through a dual focus: it examines the main nanomaterial classes reported in the design of electrochemical biosensors, while systematically considering regulatory frameworks—particularly within the European context—that govern their translation, commercialization, and market approval. Reported performance gains are contextualized with respect to specific experimental and operational parameters, including electrode geometry, measurement protocols, data treatment strategies, and background current contributions. By jointly addressing technological performance and regulatory requirements, the review identifies current translational bottlenecks and outlines a roadmap for the rational design of electrochemical biosensors that are not only analytically robust, but also positioned for feasible clinical, industrial, and environmental deployment.

2. Electrochemical Biosensor and Nanomaterials

Electrochemical biosensors are commonly classified as potentiometric (potential-based), amperometric/voltammetric (generating faradaic current under fixed or swept potentials), and impedimetric (changing in resistance and/or reactance), each class offering characteristic strengths alongside intrinsic constraints. Figure 2 summarizes the main classes and their representative applications, advantages, and limitations.

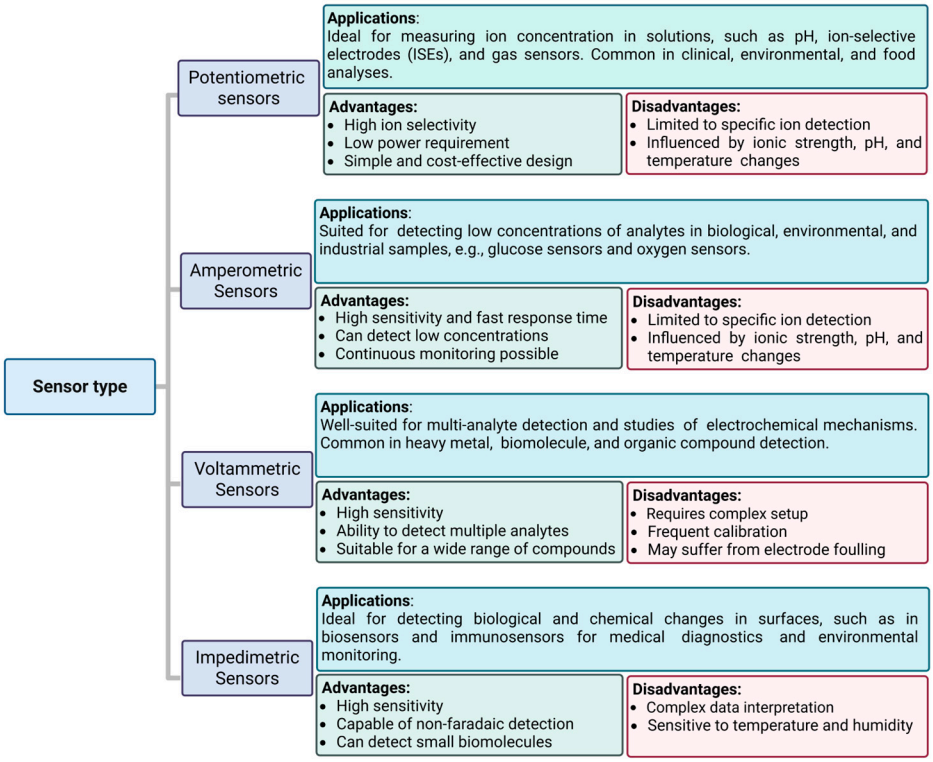

Figure 2. Comparison of various types of electrochemical sensors, their advantages, and disadvantages. Created in BioRender (Academic Publication License). Placci, A. https://BioRender.com/tpj721e (accessed on 9 February 2026).

Upon biotarget recognition—either through a catalytic process (e.g., enzyme-mediated) or a specific binding event (e.g., antibody- or aptamer-based)—the interfacial properties of the electrode are perturbed, generating an electrical signal that is quantitatively related

to analyte concentration. In such systems, nanomaterials are integrated directly at the electrode–electrolyte interface, enabling modulation of heterogeneous electron-transfer pathways, double-layer capacitance, local mass-transport regimes, and the surface density and orientation of immobilized biorecognition layers [15]. These parameters directly govern faradaic currents, impedance responses, and background noise levels. By contrast, in optical or colorimetric assays, nanomaterials more often function as distal or indirect signal amplifiers rather than as integral components of the transduction interface [16]. From a practical perspective, electrochemical biosensors offer distinct advantages for decentralized and point-of-care testing. Signal readout relies on straightforward electrical measurements that scale favorably with electrode miniaturization, operate at low power, and are compatible with planar, disposable screen-printed electrodes [17]. Consequently, device performance is dictated primarily by interfacial electrochemistry rather than by optical path length, illumination homogeneity, or alignment precision, enabling compact and cost-effective analytical platforms while preserving quantitative control over the sensing interface [16]. At the same time, key limitations arise from this very interfacial sensitivity: electrochemical signals are strongly influenced by background (capacitive) currents, matrix effects, and electrode-to-electrode variability, while reported figures of merit—particularly limits of detection (LOD)—are highly dependent on electrode geometry, surface functionalization protocols, measurement modality, and data treatment strategies. These factors frequently complicate direct comparison across studies and hinder straightforward translation.

3. Nanomaterials for Electrochemical Biosensing Applications

The development of highly sensitive, reliable, robust, portable, and cost-effective sensing strategies has become increasingly important in modern analytical science. Conventional analytical techniques often suffer from complex sample preparation, lengthy analysis times, high operational costs, and the requirement for specialized instrumentation and trained personnel [18]. The integration of nanomaterials into electrochemical biosensor design has provided a significant added value by improving key analytical figures of merit, most notably sensitivity, signal-to-noise ratio, LODs. In particular, nanocomposites and nanohybrids—comprising nanoparticles, nanotubes, MXenes, nanostructured metal–organic frameworks (MOFs)—enable the construction of tailorable architectures optimized for electrochemical signal transduction [19]. The synergistic combination of materials with complementary properties, such as high electrical conductivity, efficient electron-transfer kinetics, and intrinsic electrocatalytic activity, results in enhanced analytical performance and lower detectable concentrations of target analytes [20]. At the interface level, nanomaterials generally fulfill two primary functions: facilitating electron transfer between the biorecognition event and the electrode surface, and acting as high-surface-area support matrices for the stable immobilization of biorecognition elements, thereby increasing effective loading and improving detection limits [21]. Within this framework, the present section focuses primarily on carbon-based nanostructures and metal (gold, iron) nanoparticles, which have proven particularly effective in pushing electrochemical biosensors toward ultrasensitive detection while maintaining robustness and scalability.

3.1. Carbon Nanostructures and Graphene

The recent carbon-based literature frames nanomaterials such as CNTs, graphene/GO/rGO, and their hybrids as high-surface-area conductors and bioelectronic interfaces, enabling portable and wearable electrochemical diagnostics for connected and decentralized healthcare and environment monitoring. From a mechanistic standpoint, carbon nanomaterials are differentiated according to two roles: acting as electron-transfer (ET) mediators or “wiring” elements between redox-active biomolecules and the electrode,

and producing apparent sensitivity enhancements arising from increased electroactive area, modifications of the electrical double layer, and hybrid electrocatalytic effects in polymer/metal(oxide)/doped-carbon composites [22]. CNT-modified electrodes typically enhance electroactive surface area approximately 5-fold to over 20-fold, depending on nanotube length, bundling, and film density. Quantitative measurements based on double-layer charging currents and redox probe voltammetry (e.g., ferro/ferricyanide or ferrocene derivatives) consistently show proportional increases in faradaic current accompanied by increases in double-layer capacitance from typical values of 20–40 $\mu F\ cm^{-2}$ for planar electrodes to 150–400 $\mu F\ cm^{-2}$ for dense CNT networks [23,24]. As a result, background charging currents often increase by nearly one order of magnitude, particularly at scan rates above 50–100 $mV\ s^{-1}$, substantially affecting limits of detection when noise is properly accounted for. Several comparative studies report that while calibration slopes increase by factors of 5–10, the actual improvement in signal-to-background ratio rarely exceeds a factor of 2–3 [23,24].

In redox-enzyme-based biosensors, CNT-mediated enhancement of heterogeneous electron transfer is largely restricted to metalloenzymes with surface-accessible cofactors. A paradigmatic example is cytochrome c nitrite reductase (ccNiR) from Desulfovibrio desulfuricans, a multi-heme enzyme whose catalytic site lies adjacent to a hydrophobic surface domain. On CNT-modified electrodes, cyclic voltammetry displays quasi-reversible Fe(III)/Fe(II) redox couples with peak-to-peak separations (ΔE_p) of 70–90 mV at scan rates below 20 $mV\ s^{-1}$ and heterogeneous electron-transfer rate constants (k^0) of 10–25 s^{-1} derived from Laviron analysis [25,26]. Under catalytic conditions, steady-state nitrite reduction currents occur within $\pm$40–60 mV of the formal heme potential, consistent with kinetically competent direct electron transfer rather than diffusion-limited amplification. Notably, these systems also exhibit 5–8$\times$ increases in background currents relative to planar electrodes, indicating that higher catalytic currents do not translate proportionally into improved analytical performance. Outside such favorable structural configurations, CNTs do not intrinsically enable direct electron transfer. This limitation is particularly evident in flavoenzyme-based biosensors employing glucose oxidase (GOx). Owing to the deeply buried FAD cofactor ($\approx$12–14 Å from the protein surface), randomly adsorbed GOx on CNT films shows no resolvable FAD/$FADH_2$ redox peaks, even at low scan rates ($\leq$5 $mV\ s^{-1}$), and catalytic glucose oxidation currents remain dominated by oxygen-mediated pathways despite increased enzyme loading [27,28]. There, CNTs primarily act as high-area immobilization scaffolds rather than electronic mediators. True CNT-enabled electrical wiring of flavoenzymes has been demonstrated only in highly controlled architectures. Willner and co-workers achieved mediator-free glucose oxidation by reconstituting apo-GOx on FAD-functionalized CNTs covalently tethered to electrode surfaces, establishing direct electronic coupling between the FAD center and the electrode [27,28]. In these systems, electron-transfer turnover frequencies approaching 10^3–$10^4\ s^{-1}$ were reported, exceeding electron transfer to molecular oxygen by nearly one order of magnitude; however, performance depends critically on CNT length (<20 nm), linker flexibility, and surface density, underscoring the extreme sensitivity of such systems to nanoscale heterogeneity.

CNTs have been widely employed in field-effect transistor (FET) biosensors. CNT-based FET biosensors are often interpreted as transducing biorecognition through direct charge transfer, but mechanistic studies show that responses are dominated by electrostatic gating, Schottky barrier modulation at metal–CNT contacts, and electrical double-layer effects. Besteman et al. [29] and Patolsky et al. [28] demonstrated that ionic strength and Debye screening control signal amplitude, which collapses when the Debye length falls below ~1–2 nm.

Gazzato and Frasconi recently reported CNT-based and CNT/graphene-containing flexible electrochemical biosensors with a device-centric perspective, showing that fabrication parameters (film vs. fiber architectures, dispersion protocols, polymer matrices) critically determine not only conductivity and mechanical compliance but also signal dispersion and reproducibility [30]. Performance variability is systematically linked to nanomaterial heterogeneity, with CNT aggregation identified as a primary source of analytical uncertainty; homogeneous dispersions achieved via controlled sonication, chemical functionalization, or polymer/surfactant stabilization are required to obtain stable baseline currents and reproducible responses. This approach enables a clearer separation between genuine interfacial or kinetic improvements, such as enhanced percolation pathways, CNT alignment in fibers, while the reduced charge-transport resistance, and apparent sensitivity gains arising from increased electroactive area, hybrid composites (e.g., CNTs with metal nanoparticles, Prussian blue, or conductive polymers) increase in capacitive background currents. The broad range of analytical performances reported (LOD from sub-μM to nM/fM; linear ranges spanning 2–4 orders of magnitude across direct, enzymatic, and affinity sensors) indicates that cross-platform comparisons are only meaningful when electrode geometry, effective area, baseline subtraction, and noise models are standardized; otherwise, LOD largely reflects the measurement protocol rather than an intrinsic nanomaterial effect.

Other noteworthy graphene-derived materials include graphene oxide (GO). Pristine graphene exhibits high carrier mobility, but its basal plane is largely electrochemically inert, and biosensors rely on defect-rich rGO or multilayer graphene. Heterogeneous electron-transfer rate constants for outer-sphere redox couples increase from ~10^{-4}–10^{-3} cm s^{-1} on basal-plane graphite to ~10^{-2}–10^{-1} cm s^{-1} on rGO, correlating with defect density rather than intrinsic conductivity. These observations demonstrate that electrochemical activity in graphene-based sensors is governed by defect chemistry rather than ideal two-dimensional electronic structure [31].

CNT-based biosensors are clearly more mature than graphene-based counterparts [32], yet interest in this two-dimensional material for bioanalytical applications continues to grow. In addition to true monolayer graphene isolated by mechanical cleavage from highly oriented pyrolytic graphite (HOPG), by CVD on metal foils, or by epitaxy on silicon carbide, a broad family of graphite-derived bulk materials is commonly referred to as "graphene" [33]. As with CNTs, graphene-based materials are widely employed in FET configurations [34], where graphene is used primarily as a high-specific-surface electrode material. Overall, graphene and CNTs are the most promising carbon nanostructures for biosensing applications, each allotrope offering distinct advantages as a transduction element [20].

Additional examples of electrochemical biosensors incorporating carbon nanostructures and graphene are reported in Table 1.

Table 1. List of analytes detected by electrochemical sensors improved by carbon nanostructures.

Target	Substrate	Electrochemical Method	LOD	Refs.
DNA (hybridization, FET format)	CNT-FET with receptor bound to Au electrodes via thioethers; recognition localized on the source/drain region	FET (conductance)	N.D.	[35]
Enzymes/Immunoassay on CNT-FET	Functionalized CNT channel (enzymes/antibodies)	FET (conductance)	N.D.	[36,37]
Biomarkers (graphene electrode)	rGO/GO or graphene electrodes on a conductive substrate	CV, DPV, Amperometry, EIS	N.D.	[38,39]

3.2. Gold Nanoparticles

Among noble-metal nanomaterials, gold nanoparticles (AuNPs) are widely employed in electrochemical biosensors; the enhancement of analytical performance reported for AuNP-modified electrodes originates from geometric amplification, interfacial capacitance effects, and, in selected architectures, kinetic facilitation of heterogeneous electron transfer. AuNP-modified electrodes typically exhibit an increase in electroactive surface area by factors of 3–10 relative to bare planar electrodes, which proportionally amplifies faradaic currents but also leads to a substantial increase in double-layer capacitance and background charging currents [40].

In redox-enzyme-based biosensors, AuNP-mediated electron-transfer enhancement has been demonstrated primarily for metalloenzymes such as horseradish peroxidase (HRP). In these systems, cyclic voltammetry reveals quasi-reversible Fe(III)/Fe(II) redox couples with peak-to-peak separations below 80–100 mV and heterogeneous electron-transfer rate constants (k^0) on the order of 10–30 s^{-1}, values significantly higher than those observed on non-nanostructured electrodes [41]. Under catalytic conditions, AuNP–HRP electrodes generate steady-state reduction currents for H_2O_2 at potentials within $\pm$50 mV of the formal redox potential of the heme center, supporting the presence of kinetically competent electronic coupling rather than purely diffusion-controlled signal amplification. Importantly, these studies also report a concurrent increase in capacitive currents by up to one order of magnitude, resulting in signal-to-background ratios that depend strongly on the measurement technique and filtering strategy. As a consequence, sensitivity (often not normalized) is reported to increase by factors of 5–10, whereas the true signal-to-noise improvement is frequently limited to a factor of 2–3. This distinction highlights that gains in sensitivity reported for AuNP-based biosensors are often apparent rather than intrinsic and must be interpreted in the context of background current contributions.

The limitations of AuNP-mediated electron transfer become particularly evident in flavoenzyme-based biosensors, most notably those employing glucose oxidase (GOx). Comparative studies employing randomly adsorbed GOx on AuNP films show no resolvable FAD redox peaks and catalytic currents dominated by oxygen-mediated pathways, despite increased enzyme loading and higher apparent sensitivity [37]. In these configurations, AuNPs primarily act as high-area scaffolds rather than true electronic mediators.

In contrast, true AuNP-enabled electrical wiring of GOx has been demonstrated through the reconstitution of apo-GOx on FAD-functionalized AuNPs directly tethered to the electrode surface [42]. In this architecture, AuNPs function as nanoscale electrodes that electronically couple the FAD center to the bulk electrode, yielding oxygen-independent glucose oxidation with electron turnover rates approaching 5×10^3 s^{-1}, exceeding the rate of electron transfer to the native O_2 acceptor by nearly one order of magnitude [43]. The resulting amperometric response remains highly sensitive to nanoparticle size distribution, linker length, and surface coverage.

Beyond conventional spherical AuNPs, recent advances have explored unconventional gold nanostructures and hybrid Au-NPs to further enhance biosensor performance through combined electromagnetic and chemical mechanisms [44]. Notably, Liu et al. demonstrated that plasmonic gold substrates with engineered nanoscale morphology—termed plasmonic gold (pGOLD)—can provide near-infrared fluorescence enhancement exceeding 100-fold compared to conventional glass substrates, enabling multiplexed nucleic acid detection via fluorescence-enhanced microarray technology (FEMMAN) [45]. When combined with asymmetric reverse transcription recombinase polymerase amplification (Asy-RT-RPA), this platform achieved single-copy sensitivity for SARS-CoV-2 detection and variant discrimination, with limits of detection reaching the attomolar range (1×10^{-18} M) for viral spike proteins. Critically, the reported sensitivity improvement arises primarily from plas-

monic near-field enhancement rather than direct electron-transfer facilitation, highlighting a distinct sensing modality where AuNPs function as optical signal amplifiers rather than electrochemical mediators.

In a complementary approach, Li et al. reported the quasi-epitaxial growth of high-phase-purity 1T′-phase transition metal dichalcogenide (TMD) monolayers on 4H-phase gold nanowires (4H-Au NWs), forming core–shell 4H-Au@1T′-TMD heterostructures with ultrasensitive surface-enhanced Raman scattering (SERS) capabilities [46]. The metastable 1T′-TMD shell (e.g., WS_2, WSe_2, MoS_2, $MoSe_2$) exhibits semi-metallic properties and enhanced charge-transfer interactions with analyte molecules compared to the thermodynamically stable 2H phase, resulting in superior SERS performance. For instance, 4H-Au@1T′-WS_2 nanowires achieved attomole-level detection of Rhodamine 6G (LOD: 1×10^{-18} M) and SARS-CoV-2 spike protein variants, leveraging both electromagnetic field enhancement from the plasmonic Au core and chemical enhancement from efficient charge transfer at the 1T′-WS_2 shell. The ultrathin (~0.6 nm) semi-metallic shell allows strong electromagnetic coupling while maintaining high chemical reactivity, representing a synergistic integration of plasmonic and 2D-material-based sensing mechanisms. However, reproducibility and long-term phase stability of 1T′-TMD shells under operational conditions, as well as scalability of the wet-chemical synthesis protocol, are required prior to translating these architectures into robust analytical platforms.

Both studies underscore that advanced Au-based nanoarchitectures can achieve unprecedented sensitivity through mechanisms beyond conventional electrochemical signal transduction—namely, plasmonic fluorescence enhancement and SERS-mediated chemical detection. Nevertheless, these modalities introduce additional complexity in terms of instrumentation requirements, signal interpretation, and interlaboratory reproducibility, factors that must be carefully addressed in the context of regulatory validation and commercial deployment.

Additional examples of electrochemical biosensors incorporating gold nanoparticles are summarized in Table 2.

Table 2. List of analytes detected by electrochemical sensors improved by AuNPs.

Target	Substrate	Electrochemical Method	LOD	Ref.
E. coli O157:H7 (aptasensor)	rGO–PVA/AuNP-modified GCE; anti-*E. coli* aptamer	DPV	9.34 CFU/mL	[47]
SARS-CoV-2 spike (immunosensor)	SPCE with electrodeposited AuNP; anti-S antibody	EIS	3.16 pmol/L	[48]
Aflatoxin B1 (immunosensor)	GCE/poly(thionine) with AuNP; anti-AFB1	DPV	0.07 ng/mL	[49]
Procalcitonin (immunosensor)	Laser-engraved graphene interdigitated electrode decorated with AuNP	EIS	0.36 pg/mL	[50]
PfHRP2 malaria (immunosensor)	Screen-printed Au electrodes; AuNP-amplified Ab-HRP	Amperometry	36 pg/mL	[51]
Salmonella (*S. enteritidis*) (aptasensor)	AuNP-modified SPCE; SELEX aptamer	EIS	600 CFU/mL	[52]
Glucose (GOx wiring)	Au electrode with FAD-modified AuNP–reconstituted apo-GOx	CV—chronoamperometry	N.D.	[27]
Catechol (CC)	Lac/GC@B_4C/AuNPs/NF (laccase immobilized on GC@B_4C with electrodeposited AuNPs on nickel foam)	Chronoamperometry	25 nM	[53]
TGF-α (cytokine, immunosensor)	Functionalized SPCE modified with low-dimensional Au nanomaterials	CV	0.35 pg/mL	[54]

3.3. Iron-Based Magnetic Nanoparticles

Iron-based magnetic nanoparticles (MNPs), particularly Fe_3O_4 and iron-oxide derivatives, are extensively used in electrochemical biosensors; however, a mechanistic analysis shows that reported improvements (e.g., in LOD and sensitivity) are predominantly driven by magnetically assisted mass-transport control and signal amplification, rather than by intrinsic enhancement of heterogeneous electron-transfer kinetics. In most MNP-based platforms, cyclic voltammetry reveals no significant reduction in peak-to-peak separation or shift in formal potentials upon MNP incorporation, indicating that electron-transfer rates at the electrode interface remain largely unchanged [55–57].

Electrochemical impedance spectroscopy (EIS), frequently invoked as evidence of kinetic enhancement, must therefore be interpreted with caution. In porous Fe_3O_4-based architectures, apparent decreases in charge-transfer resistance (Rct) typically originate from increased electroactive surface area and improved ionic accessibility rather than from accelerated electron transfer. Impedance spectra collected over broad frequency windows (10^5–10^{-1} Hz) are best fitted using Randles-type equivalent circuits incorporating constant-phase elements (CPEs), reflecting significant interfacial heterogeneity. In these cases, variations in the CPE exponent and Warburg impedance dominate the analytical response, underscoring that sensitivity gains arise from modified interfacial transport and capacitance rather than from true kinetic acceleration [58,59].

A representative example of this mechanism is provided by the DNA-capped porous Fe_3O_4 system reported by Cui and co-workers, where ultrasensitive Hg^{2+} detection (LOD $\approx$ 3.2 pM) is achieved via target-triggered release of encapsulated $[Fe(CN)_6]^{3-}$ redox mediators. In this architecture, voltammetric signals emerge only after pore opening, while EIS analysis confirms that sensing is governed by mediator availability. Importantly, explicit reporting of background currents, impedance fitting parameters, and long-term signal retention (>90% after 30 days) enables a realistic assessment of robustness and analytical uncertainty [60].

A complementary interface sensing strategy is illustrated by the label-free atrazine immunosensor reported by Zumpano et al., based on protein G-functionalized magnetic nanoparticles (MNPs@protG, ~300 nm) magnetically confined onto a highly porous gold screen-printed electrode modified with a Prussian Blue (PB) thin film acting as an internal redox probe. In this system, MNPs enable oriented antibody immobilization and spatial confinement while preserving interfacial conductivity through the porous Au scaffold. Electrochemical characterization demonstrates that sensitivity enhancement arises from interfacial transport modulation: cyclic voltammetry confirms a $>10^3$-fold increase in electroactive surface area, while differential pulse voltammetry shows progressive attenuation of the PB anodic peak upon MNP deposition, antibody binding, and antigen recognition. This signal decrease is mechanistically attributed to restricted K^+ ion exchange within the PB lattice and increased interfacial capacitance, with no measurable shifts in formal potentials or peak-to-peak separations. The reported low LOD (0.011 ng mL^{-1}) and wide linear range (0.05–1.5 ng mL^{-1}), together with electrode-to-electrode reproducibility below 5% and long-term signal stability exceeding 90%, highlight that analytical robustness is governed by nanostructure and magnetic confinement rather than intrinsic MNP electroactivity [61].

At this point, the role of nanomaterial heterogeneity becomes critical. Iron-oxide MNPs often exhibit broad size distributions (≈100–300 nm) and variable porosity, which directly propagate into electrode-to-electrode variability. Polymer- or polydopamine-coated Fe_3O_4 cores mitigate aggregation and surface inhomogeneity, yielding relative standard deviations below 5–8%, whereas uncoated systems frequently exceed 15%, highlighting the direct link between MNP heterogeneity and analytical uncertainty [62].

A further example of blocking-dominated signal transduction is provided by the magnetic nanoparticle-assisted electrochemical platform for methylated SEPT9 DNA detection reported by Hanoglu et al. In this system, ferrocene-labeled PNA probes immobilized on antibody-functionalized Fe_3O_4 nanoparticles are magnetically confined onto screen-printed carbon electrodes, where MNPs act as magnetic concentrators and spatial organizers rather than as electron-transfer mediators. Cyclic voltammetry and EIS show progressive attenuation of ferrocene redox currents and increased Rct upon biofunctionalization and target binding, consistent with interfacial insulation effects. Impedance spectra are fitted using Randles-type equivalent circuits, confirming that signal modulation arises from steric blocking and transport limitation rather than from enhanced electron-transfer kinetics. Differential pulse voltammetry provides the analytical readout, with a reported LOD of 0.37% methylation and a linear range of 25–100%, while reproducibility (RSD < 5%) reflects controlled nanoparticle functionalization and magnetic confinement [63].

Overall, these studies collectively demonstrate that iron-based MNPs enhance electrochemical biosensor performance primarily through spatial organization of bioreceptors, magnetically assisted mass transport, and interfacial transport modulation, while genuine electron-transfer acceleration is rare and highly system-dependent. These findings further emphasize the necessity of explicitly reporting background currents, impedance modeling assumptions, nanoparticle size distributions, and reproducibility metrics when interpreting analytical figures of merit in MNP-based sensing platforms.

Additional examples of electrochemical biosensors incorporating iron-based magnetic nanoparticles are summarized in Table 3.

Table 3. List of analytes detected by electrochemical sensors improved by MNPs.

Target	Substrate	Electrochemical Method	LOD	Ref.
Glucose	Pt/GOD/Fe_3O_4 nanoparticles/chitosan (Cs)/Nafion-modified Pt electrode	Amperometry	6×10^{-6} M	[58]
Carcinoembryonic antigen (CEA); α-Fetoprotein (AFP)	Gold electrode modified with chitosan–nanoAu hydrogel and anti-AFP and anti-CEA antibody; sandwich detection using (GOD + HRP)-Au–PB–Fe_3O_4-labeled secondary antibody	CV	7 pg/mL	[59]
Na^+ storage	Fe_2O_3 nanoparticles anchored on N-doped graphene (Fe_2O_3/N-graphene) electrode	CV	N.D.	[49]
CXCL9 (protein biomarker)	SPCE with cAb-MNPs and dually labeled AuNPs	Chronoamperometry	27 pg/mL	[64]

3.4. Critical Assessment of Analytical Performance Parameters in Nanomaterial-Based Electrochemical Biosensors

While nanomaterial-modified electrodes consistently report improved analytical performances—including enhanced sensitivity and reduced LOD—direct quantitative comparison across different platforms remains challenging due to substantial variability in electrode geometry, surface modification protocols, measurement techniques, and data treatment methods [65]. Accordingly, this section aims to contextualize the LOD values reported in Table 2 and in Table 3 by critically examining how these experimental and analytical parameters influence the reported performance metrics and their effective comparability. It should be noted that the studies summarized in Table 1 are not discussed here in terms of LOD, as the corresponding reference articles did not explicitly report detection limits. Nevertheless, the considerations outlined in this section are equally applicable to those systems, including CNT- and graphene-based architectures, and more broadly to any electrochemical biosensor incorporating nanomaterials as functional components.

Electrode geometry. Electrode geometry plays a decisive role in governing both absolute current responses and signal-to-background ratios in electrochemical biosensing. Planar macroelectrodes, such as screen-printed carbon electrodes (SPCEs) with relatively large geometric areas (e.g., 12.56 mm^2), enable high absolute currents and straightforward signal readout, as demonstrated by Qaanei et al. using rGO–PVA/AuNP-modified electrodes for *E. coli* O157:H7 detection [47]. However, such configurations are sensitive to electrode-to-electrode variability arising from screen-printing inhomogeneities and manual nanomaterial deposition. A similar trade-off is observed for screen-printed gold electrodes (SPGEs), which benefit from well-defined gold electrochemistry and reproducible electrodeposition of AuNPs, as shown by Brazaca et al. for SARS-CoV spike protein sensing, yet may suffer from limited nanoparticle coverage when short deposition times are employed [48]. A comparable geometry-dependent behavior is observed in the AuNP-modified SPCE immunosensor for TGF-α reported by Gaba and Jain [54], where a working electrode area of approximately 7 mm^2 (3 mm diameter) enabled sufficiently high absolute currents while maintaining compatibility with antibody immobilization and disposable point-of-care formats. In this case, electrodeposition of AuNPs on a planar SPCE resulted in a measurable increase in baseline current (from 0.50 to 0.60 mA), confirming enhanced electron-transfer kinetics, while preserving geometric simplicity and reproducibility inherent to screen-printed platforms. Alternative geometries aim to enhance mass transport and interfacial reactivity. Laser-engraved graphene interdigitated electrodes, with high edge-plane-to-basal-plane ratios and reduced diffusion distances, have been shown to improve sensitivity, as reported by Amouzadeh Tabrizi and Acedo for procalcitonin detection [50]. Nevertheless, interdigitated designs introduce additional complexity in defining the effective electroactive area and in comparing performance metrics with conventional planar electrodes. Conversely, the use of smaller-area electrodes, such as 3 mm glassy carbon disks modified with polythionine and electrodeposited AuNPs for aflatoxin B1 immunosensing, reduces absolute currents but can improve reproducibility and minimize reagent consumption [49]. Electrode size and geometry also influence the feasibility of multilayer architectures. Larger gold electrodes (e.g., 12.56–19.6 mm^2) facilitate the sequential integration of polymer films, AuNPs, antibodies, and magnetic labels, as demonstrated in sandwich immunosensors for CEA, AFP, and PfHRP2 detection [59], but each additional modification step represents a potential source of variability affecting interfacial charge transfer and, in the case of impedimetric readouts, the measured resistance spectrum [51]. In contrast, miniaturized noble-metal electrodes, such as 1 mm platinum disks used for glucose biosensing with Fe_3O_4 NPs, GOD, chitosan, and Nafion, offer well-defined electrochemistry and reproducible enzyme immobilization, albeit at the expense of lower absolute currents [58]. Collectively, these examples highlight that electrode geometry is a central factor that mediates sensitivity, reproducibility, and interpretability across electrochemical platforms.

Measurement protocols. Measurement protocols differ substantially across studies, further complicating direct quantitative comparison of analytical performance. Voltammetric and amperometric techniques are frequently employed for signal transduction, yet they probe distinct aspects of the electrode–interface system and are characterized by different susceptibilities to noise and mass-transport effects. For example, Qaanei et al. employed differential pulse voltammetry (DPV) using a TMB–H_2O_2–HRP amplification system at a scan rate of 50 mV s^{-1}, exploiting the inherent background suppression of pulsed techniques to enhance sensitivity [47]. In contrast, Brazaca et al. and Owino et al. relied on chronoamperometry at fixed potentials (–200 mV and –175 mV, respectively) for SARS-CoV spike protein and aflatoxin B1 detection [49], prioritizing temporal simplicity and direct current readout at the expense of increased susceptibility to baseline drift and capacitive contributions [48]. Impedimetric approaches introduce an additional layer of

complexity. Amouzadeh Tabrizi and Acedo recorded electrochemical impedance spectra over a broad frequency range (100 kHz to 0.1 Hz) using a small AC perturbation (10 mV), whereas Hemben et al. and Labib et al. employed the same frequency window but with a substantially larger amplitude (0.25 V) for PfHRP2 and *Salmonella enteritidis* sensing, respectively [50–52]. Such differences in excitation amplitude and fitting strategy can significantly alter the apparent charge-transfer resistance and, consequently, the derived sensitivity and LOD. Amperometric biosensing under enzymatic control provides further illustration of protocol-dependent performance. Similarly, in the AuNP-modified SPCE immunosensor for TGF-α, cyclic voltammetry was employed as the primary transduction technique using a ferri/ferrocyanide redox probe over a wide potential window (−1 to +1 V) at moderate scan rates (50 mV s^{-1}). This choice emphasizes interface-controlled charge-transfer modulation induced by antibody–antigen binding, rather than catalytic signal amplification, resulting in a signal-suppression-based detection mechanism that is inherently sensitive to surface coverage and protein layer formation. Yang et al. performed glucose detection at a fixed potential of –0.4 V (vs. Ag/AgCl) in phosphate buffer (pH 6.8) at 35 °C, recording steady-state currents upon successive glucose additions to obtain a wide linear range (6×10^{-6} to 2.2×10^{-3} M) and a detection limit of 6×10^{-6} M, defined at a signal-to-noise ratio of 3 [58]. In contrast, Zhuo et al. employed cyclic voltammetry at 50 mV s^{-1} over a potential window of −0.2 to 0.6 V (vs. SCE) in glucose-containing buffer to exploit the catalytic amplification provided by HRP and GOD co-functionalized on Au–PB–Fe_3O_4 magnetic nanoparticles, achieving ultralow detection limits for CEA (4 pg mL^{-1}) and AFP (7 pg mL^{-1}) across broad linear ranges [59]. Collectively, these examples demonstrate that variations in electrochemical technique, potential or frequency window, excitation parameters, and signal acquisition strategies profoundly affect signal-to-noise ratios, temporal resolution, and sensitivity to interfacial changes, rendering direct quantitative comparison of reported limits of detection and linear ranges across studies nontrivial.

Background current. Background current contributions represent a critical yet often underreported factor in the evaluation of electrochemical biosensor performance. Capacitive charging currents, non-Faradaic processes, and residual electroactive impurities in buffers or biological matrices can vary substantially with electrode material, surface chemistry, and nanomaterial loading, thereby directly affecting signal-to-noise ratios and the apparent limit of detection. Carbon-based electrodes, particularly graphene-derived materials, typically exhibit higher background currents than noble-metal electrodes due to their large electroactive surface area and high double-layer capacitance, as observed for graphene-based platforms [50]. While the incorporation of metallic nanoparticles such as AuNPs often lowers overpotentials and improves apparent electron-transfer kinetics, their high surface area can concomitantly increase capacitive currents, partially offsetting gains in analytical sensitivity. In [65], the progressive decrease in current observed after antibody immobilization, blocking with albumin, and antigen binding directly reflects the formation of insulating protein layers rather than changes in faradaic reaction pathways. While AuNP deposition initially increased the current due to accelerated electron transfer, the subsequent suppression highlights the dominant contribution of non-faradaic and capacitive effects associated with biomolecular surface coverage, underscoring the importance of distinguishing true analytical signals from background modulation in protein-based biosensors. Similar considerations apply to iron oxide nanoparticles. Fe_3O_4 NPs exhibit intrinsic peroxidase-like activity and can catalyze the reduction of H_2O_2, providing effective signal amplification but also increasing background currents through non-specific catalysis of residual peroxide or other electroactive species. In this context, Yang et al. reported a sevenfold increase in glucose oxidation current at 4 mM glucose upon Fe_3O_4 NP incorporation, attributed to their dual function as electron-transfer mediators and artificial peroxidase

catalysts [58]. However, the absence of quantitative signal-to-background ratios or relative standard deviations of blank measurements limits assessment of the true robustness of the reported detection limit. Multicomponent nanohybrids further complicate background current contributions. Zhuo et al. demonstrated that three-layer Au–PB–Fe_3O_4 magnetic nanoparticles exhibited pronounced redox activity, with well-defined cyclic voltammetric peaks at 0.18 and 0.24 V (vs. SCE) arising from the Prussian Blue interlayer acting as an "artificial peroxidase" mediator [59]. While this architecture enhances electron transfer between enzymes and the electrode, the intrinsic electroactivity of Prussian Blue introduces additional background currents that must be carefully deconvoluted from analytically relevant signals. Collectively, these studies underscore that limits of detection derived solely from absolute current changes, without explicit consideration of background current contributions, risk overestimating true analytical performance. The lack of systematic reporting of signal-to-background ratios and blank variability across different surface modification strategies remains a significant limitation for rigorous cross-platform comparison of LOD values.

Data treatment. Data treatment and reporting practices introduce an additional and often underestimated source of variability in the evaluation of analytical performance. Most studies calculate the LOD using the conventional $3\sigma/S$ criterion, where σ represents the standard deviation of blank measurements and S the slope of the calibration curve. However, both the number of blank replicates and the definition of the "blank" itself vary widely across studies, ranging from buffer-only controls to non-target proteins or complex biological matrices (from [47–50]), thereby limiting the comparability of reported LOD values. Matrix effects are particularly illustrative of this issue. Brazaca et al. reported LODs in both buffer and spiked human serum, showing consistently higher values in serum (2.95 ng mL^{-1} without amplification and 40 pg mL^{-1} with AuNP amplification) compared to buffer (2.14 ng mL^{-1} and 36 pg mL^{-1}, respectively), underscoring the impact of nonspecific interactions and background contributions that are often overlooked when LODs are determined exclusively in idealized media [48]. For instance, in the AuNP-based TGF-α immunosensor, the limit of detection (0.35 pg mL^{-1}) was calculated using the conventional 3 σ/m criterion, where σ was derived from replicate blank measurements and m from the slope of the calibration curve obtained over a wide concentration range (1–1000 pg mL^{-1}). Notably, the calibration was performed in buffer rather than in complex biological matrices, which, while enabling precise assessment of intrinsic sensor sensitivity, may underestimate matrix-induced background contributions relevant to clinical deployment. In contrast, Yang et al. validated their Fe_3O_4 NP-based glucose biosensor directly in human serum, demonstrating good agreement with an automated biochemical analyzer (relative standard deviations of −2.97%, −1.78%, and 2.23%), a level of cross-validation that remains uncommon in the biosensor literature [58]. The treatment of calibration data further influences apparent performance. Zhuo et al. reported ultralow LODs for CEA (4 pg mL^{-1}) and AFP (7 pg mL^{-1}) across linear ranges spanning nearly four orders of magnitude by exploiting bienzyme catalytic amplification in glucose-containing media [59]. While these results highlight the power of signal amplification strategies, they also emphasize the importance of reporting stabilized rather than initial response metrics, a concept well recognized in electrochemical energy-storage studies. Finally, inconsistencies in data extraction from impedance measurements further complicate comparison. Some studies derive LODs from absolute charge-transfer resistance (Rct), whereas others rely on ΔRct (the change in Rct upon target binding). Although the former approach simplifies assay implementation by requiring a single measurement, it is more sensitive to electrode-to-electrode variability, while the latter offers a more robust representation of specific binding at the cost of increased experimental uncertainty [50–52]. Taken together, these examples demonstrate

that differences in data treatment, blank definition, matrix selection, and performance metric extraction can substantially bias reported limits of detection, reinforcing the need for standardized and transparently reported analytical protocols.

In summary, while AuNP-based and magnetic iron oxide NP-based electrochemical biosensors consistently report improved analytical performance, direct comparison of LOD values across platforms is severely hindered by variability in electrode geometry, measurement protocols, background current contributions, data treatment, nanoparticle synthesis and deposition conditions (including Fe_3O_4 NP coprecipitation methods, size control, surface functionalization with Prussian Blue or nitrogen-doped graphene, and magnetic separation protocols), and biorecognition element immobilization. To enable reproducible and transferable biosensor development, future studies should explicitly report electrode geometry and effective surface area, nanoparticle synthesis and deposition protocols (including coprecipitation conditions, surface modifications, and magnetic properties), signal-to-background ratios, blank replicates and definitions, total versus differential signal measurements, matrix validation in relevant biological samples, and biorecognition immobilization chemistry and surface coverage. Only through standardized reporting practices can nanomaterial-enhanced electrochemical biosensors advance toward clinically and industrially deployable analytical tools.

4. Integration of Nanomaterials in Electrochemical Biosensing Devices: Regulatory Frameworks

Although nanomaterial-enhanced electrochemical sensors are the focus of intense academic research, they remain far from reaching the horizon of market approval [21]. A critical gap exists between laboratory-scale performance metrics and regulatory requirements for market entry, representing a substantial barrier to the bench-to-market transition. On the laboratory bench, biosensor performance is typically evaluated through LOD, linear range, sensitivity, and selectivity—parameters that demonstrate analytical capability under idealized conditions. However, regulatory frameworks focus on entirely different criteria: batch-to-batch reproducibility, long-term stability under real-world storage and operational conditions, metrological traceability of measurements, and—crucially for nanomaterial-based devices—comprehensive physicochemical characterization, toxicological screening, and safe exposure levels. Consequently, the remarkable analytical enhancements provided by nanomaterials—which are often referred to as 'game changers' due to their ability to drastically modify sensor performance through variations in size, morphology, composition, and electrochemical properties—actually introduce additional regulatory complexity. On one hand, variations in nanomaterial properties affect final sensor performance so profoundly that compliance with existing regulatory frameworks becomes more challenging; on the other, the substantial performance improvements enabled by nanomaterials should serve as the driving force toward the establishment of specific, tailored regulatory frameworks for this emerging class of devices [20]. Therefore, successful bench-to-market transition requires not only demonstration of superior analytical performance but also rigorous validation of reproducibility, traceability, stability, and safety according to harmonized international standards.

Definition of Nanomaterials. The regulatory assessment of any nanomaterial-enhanced electrochemical biosensor must begin with the definition of a nanomaterial. In 2022, the European Commission, through the Scientific Committee on Emerging and Newly Identified Health Risks (SCENIHR) and the Joint Research Centre (JRC), revised the Recommendation 2011/696/EU concerning the definition of a nanomaterial. Establishing the range of 1–100 nm implies that a limited number of materials are formally considered nanomaterials; for instance, nanotubes with diameters below 1 nm and lengths exceeding 100 nm

would technically fall outside this range. To address this potential omission, Recommendation 2011/696/EU explicitly includes as nanomaterials fullerenes, graphene flakes, and single-walled carbon nanotubes with one or more external dimensions below 1 nm. It is expected that scientific and technological progress will generate additional analogous materials, requiring periodic and continuous updates to the scope of the definition. This legal definition directly impacts regulatory classification: a biosensor incorporating gold nanoparticles of 50 nm diameter is unambiguously subject to nanomaterial-specific regulations, whereas a biosensor using graphene nanosheets may require case-by-case assessment to determine whether the material meets the formal definition and thus triggers additional regulatory requirements.

Physicochemical Characterization of Nanomaterials. The ISO/TC 229 Technical Committee represents the core normative framework for nanomaterials and nanomaterial-enabled devices. ISO/TR 13014 provides comprehensive guidance on the physicochemical characterization of engineered nanomaterials, specifying the Critical Quality Attributes (CQAs) that must be measured and controlled throughout production [66]. These include primary particle size and size distribution, morphology (shape, aspect ratio), crystallinity (phase composition, degree of crystallinity), specific surface area, surface chemistry and functional group density, presence and composition of coatings or surface modifiers, purity and identification of impurities, state of aggregation and agglomeration, ζ-potential (surface charge), temporal stability under storage conditions, stability in physiologically relevant media, and solubility or dissolution rate. For electrochemical biosensors incorporating gold nanoparticles, carbon nanotubes, or graphene, these parameters directly influence electrochemical performance: particle size distribution affects electroactive surface area and thus sensitivity; surface chemistry determines biorecognition element immobilization efficiency and orientation; aggregation state impacts electrode-to-electrode reproducibility; and temporal stability governs shelf life and operational lifetime. The preferred techniques for particle size determination are Dynamic Light Scattering (DLS) and Transmission Electron Microscopy (TEM), standardized in ISO 22412:2025 and ISO 21363:2020, respectively [67,68]. ISO 17200 provides additional guidance for nanoparticles in powder form, addressing issues such as sample preparation, dispersion protocols, and measurement repeatability [69]. Importantly, ISO/TR 13014 emphasizes that all measurements must be accompanied by declared measurement uncertainty, calculated according to the Guide to the Expression of Uncertainty in Measurement (GUM), and that results must be traceable to SI units through the use of certified reference materials (CRMs) produced in accordance with ISO 17034 [70]. For a nanomaterial-enhanced electrochemical biosensor, complete physicochemical characterization is mandatory regardless of the intended application; toxicological screening, however, may be required or waived depending on the level of human exposure anticipated under reasonably foreseeable conditions of use.

Toxicological Screening and Risk Assessment. ISO/TR 16197 compiles and describes toxicological screening methods for engineered nanomaterials, providing a systematic framework for preliminary hazard assessment [71]. This technical report covers in vitro cytotoxicity assays (e.g., MTT, LDH release), genotoxicity screening (e.g., Ames test, comet assay), inflammatory response assessment (e.g., cytokine release profiling), and oxidative stress evaluation (e.g., reactive oxygen species generation). For electrochemical biosensors, toxicological screening is not universally required; rather, the extent of testing depends on the anticipated route and level of human exposure. If the biosensor is classified as a medical device or in vitro diagnostic device, the ISO 10993 series of standards governs biological evaluation. ISO 10993-1 provides a risk-based framework for selecting appropriate biocompatibility tests based on the nature and duration of tissue contact [72]. ISO 10993-5 specifies in vitro cytotoxicity testing protocols [73], while ISO 10993-10 addresses irritation

and sensitization testing [74]. For nanomaterial-enhanced biosensors, particular attention must be paid to nanomaterial-specific toxicological endpoints, including size-dependent cellular uptake, biopersistence, potential for translocation across biological barriers, and immunological responses. The EFSA Guidance on Risk Assessment of Nanomaterials (2018, updated 2021) is relevant when the sensor enters into contact with food, is used for in situ food quality control, or is integrated into intelligent packaging systems [75,76]. This guidance requires: (i) complete physicochemical characterization (primary particle size, aggregation state, solubility, dissolution kinetics), (ii) assessment of nanomaterial release (migration from the sensor, abrasion during use, electrochemical degradation), (iii) toxicokinetic evaluation (absorption, distribution, metabolism, excretion) if release is demonstrated, and (iv) tiered toxicity testing (in vitro screening followed by in vivo studies if necessary). The EFSA framework explicitly recognizes that nanomaterial toxicity cannot be inferred solely from bulk material properties and that nanoscale-specific physicochemical characteristics (e.g., surface reactivity, aggregation behavior) profoundly influence biological interactions.

Regulatory Frameworks for Medical Devices and In Vitro Diagnostics. If a nanomaterial-enhanced electrochemical biosensor is intended for medical or in vitro diagnostic (IVD) use, it must comply with the Medical Device Regulation (MDR) (EU) 2017/745 and the In Vitro Diagnostic Regulation (IVDR) (EU) 2017/746, respectively [77,78]. The MDR pays specific attention to the risks associated with nanomaterials and introduces Rule 19, which details the application of the General Safety and Performance Requirements (GSPR) for devices incorporating nanomaterials according to the level of patient exposure. Under Rule 19, devices are classified into higher risk classes if they contain nanomaterials that: have a high or medium potential for internal exposure, are intended to be introduced into the human body, or could lead to long-term exposure. This classification triggers additional requirements, including enhanced clinical evaluation, stricter post-market surveillance, and mandatory notification of nanomaterial composition to competent authorities. Importantly, the IVDR (Article 10) requires that devices incorporating nanomaterials undergo a case-by-case evaluation of the nanomaterial component, considering its physicochemical properties, intended use, and potential for release or exposure during use. The IVDR defines the Performance Evaluation Report (PER) (Article 56 and Annex XIII), which comprises two main components: analytical performance (including LOD, LOQ, linearity, precision, accuracy, and critically, comprehensive nanomaterial characterization) and clinical performance (diagnostic sensitivity and specificity, positive and negative predictive values). The PER must explicitly address how nanomaterial variability (batch-to-batch differences in size distribution, surface chemistry, or aggregation state) affects analytical performance and whether such variability remains within acceptable limits defined by the clinical intended use.

Quality Management, Risk Management, and Metrological Traceability. The quality and safety of any device—including biosensors incorporating nanomaterials—are verified through compliance with international standards. ISO 13485:2016 ensures that the Quality Management System (QMS) is aligned with regulatory expectations and specifically addresses the control of manufacturing processes, acceptance criteria for incoming nanomaterial batches, validated cleaning and sterilization procedures, environmental monitoring during production, and traceability from raw material supplier to finished device [79]. ISO 14971:2019 governs risk management and requires a systematic process for identifying hazards (including nanomaterial-specific hazards such as unintended aggregation, surface degradation, or cytotoxicity), estimating risks (considering both probability and severity of harm), implementing risk controls (e.g., protective coatings to prevent nanomaterial release), and evaluating residual risks against benefit-risk criteria [80]. Tests and calibrations must be performed using validated methods in laboratories accredited

under ISO/IEC 17025, which requires demonstration of technical competence, use of validated methods with documented performance characteristics (precision, trueness, LOD, linear range, robustness), metrological traceability to the International System of Units (SI) through an unbroken chain of calibrations, and declaration of measurement uncertainty for all reported results [81]. Certified reference materials (CRMs) produced in accordance with ISO 17034 must be employed to establish calibration curves and validate measurement procedures [70]. For nanomaterial-enhanced biosensors, this means that not only must the final device output (e.g., current response) be traceable to SI units (amperes), but also that the properties of the nanomaterial component (e.g., particle size, surface area, concentration) must be traceable to SI units using nanomaterial-specific CRMs. The lack of widely available, matrix-matched nanomaterial CRMs represents a significant barrier to achieving full metrological traceability for nanomaterial-enhanced biosensors and is an area of active international standardization effort.

All regulatory frameworks discussed in this paragraph are summarized in Table 4.

Table 4. Summary of key regulations and standards relevant to nanomaterials in electrochemical biosensing.

Physicochemical Characterization of Nanomaterials	
Standard	Brief description
• ISO/TR 13014	Guidance on physicochemical characterization of engineered nanomaterials, encompassing Critical Quality Attributes (CQAs).
• ISO 22412:2025	Size determination of nanoparticles by Dynamic Light Scattering (DLS).
• ISO 21363:2020	Size and morphology analysis of nanoparticles by Transmission Electron Microscopy (TEM).
Toxicological Screening and Risk Assessment	
Standard	Brief description
• ISO/TR 16197	List and description of toxicological screening methods for nanomaterials.
• ISO 10993-1	Risk-based framework for biological evaluation of medical devices.
• ISO 10993-5	In vitro cytotoxicity testing for medical devices.
• ISO 10993-10	Irritation and sensitization testing for medical devices.
Regulatory Frameworks for Medical Devices and In Vitro Diagnostics	
Standard	Brief description
• MDR (EU) 2017/745	Regulation on medical devices, includes specific requirements for nanomaterials (Rule 19).
• IVDR (EU) 2017/746	Regulation on in vitro diagnostic medical devices, requires analytical and clinical performance evaluation.
Quality Management, Risk Management, and Metrological Traceability	
Standard	Brief description
• ISO 13485:2016	Quality management system for medical devices.
• ISO 14971:2019	Risk management for medical devices.
• ISO/IEC 17025	Requirements for technical competence of testing and calibration laboratories.
• ISO 17034	Requirements for production of certified reference materials.

Electrochemical figures of merit remain essential for early-stage sensor development; however, effective market translation of nanomaterial-based biosensors requires a broader validation paradigm in which technical performance metrics and regulatory requirements are not treated as sequential or independent constraints, but are actively co-developed. As summarized in Figure 3, only by promoting the coexistence and mutual alignment of electrochemical design parameters with regulatory frameworks can electrochemical biosensors truly transition from laboratory proof-of-concept demonstrations to reproducible, safe, and compliant analytical devices suitable for clinical, industrial, and environmental deployment.

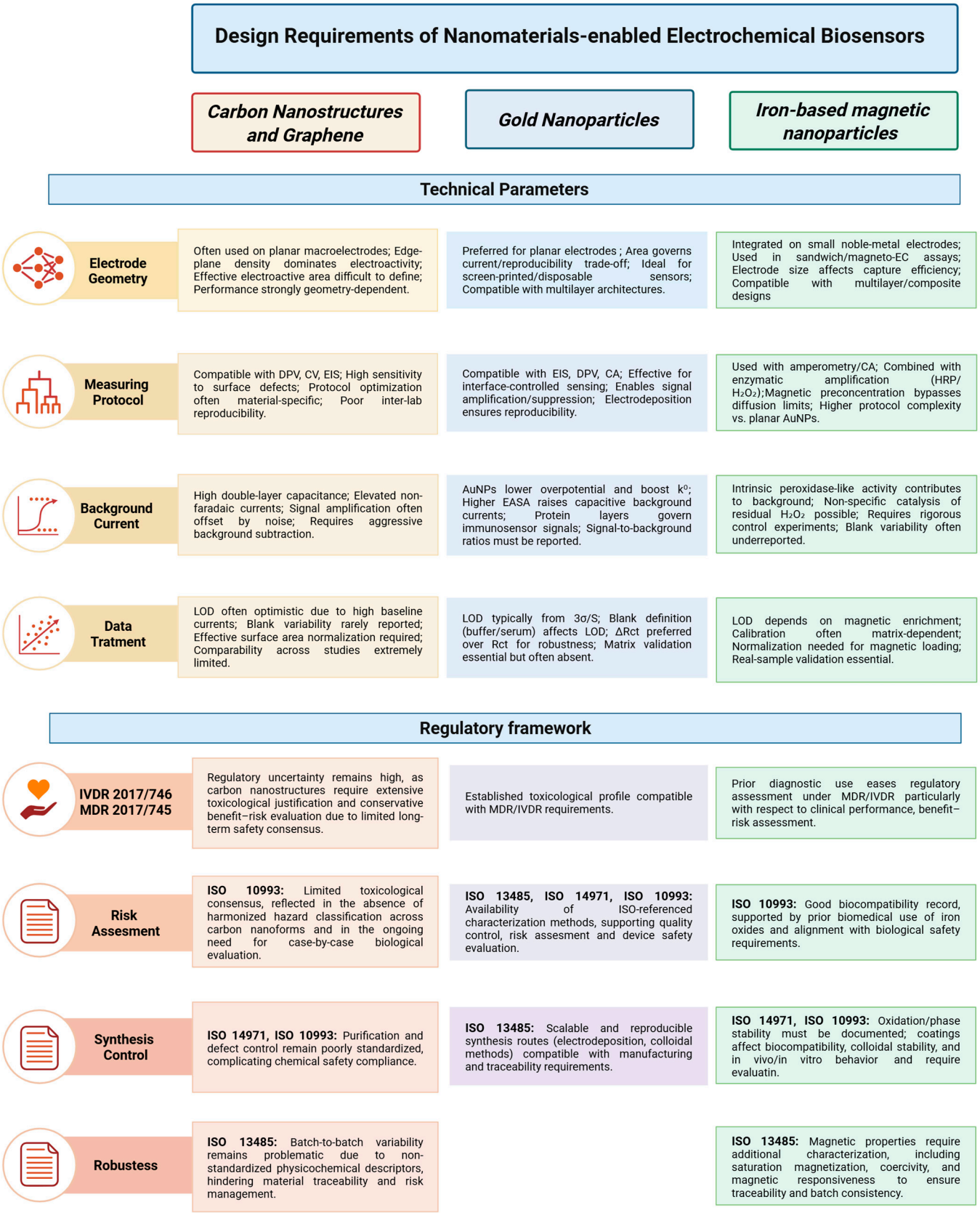

Figure 3. Integrated overview of design requirements for nanomaterial-enabled electrochemical biosensors. For each nanomaterial class, the upper panels summarize the most relevant design considerations; the lower panels report the corresponding relevant ISO standards and material-specific regulatory considerations. Created in BioRender (Academic Publication License). Rondinini, V. https://BioRender.com/3yiiv0d (accessed 9 February 2026).

5. Conclusions

Nanomaterials have fundamentally reshaped electrochemical biosensors by enhancing electron transfer, biorecognition, and signal amplification; however, these analytical gains have not translated into proportional commercial success. This gap reflects nanomaterial variability, toxicological concerns, scalability constraints, and the stringent European regulatory framework (MDR, IVDR, EFSA, ISO standards).

To bridge laboratory innovation and market deployment, nanomaterial selection must prioritize manufacturability and regulatory readiness alongside performance. Among the classes reviewed,

- Carbon nanostructures (CNTs, graphene) deliver outstanding electrochemical performance but suffer from batch-to-batch heterogeneity, complex purification, and limited toxicological consensus, restricting their use to applications where extreme sensitivity justifies regulatory complexity.
- AuNPs offer the most favorable regulatory profile owing to their often spherical morphology, controlled synthesis, extensive toxicological data, and compatibility with large-scale production, making them particularly suited for point-of-care diagnostics.
- Iron-based magnetic nanoparticles similarly benefit from strong biocompatibility records and straightforward functionalization, although their susceptibility to oxidation necessitates rigorous stability control.
- Emerging nanomaterials, including MXenes and hybrid nanocomposites and MOFs offer attractive compromises but incur increased characterization and documentation burdens, while diamond-based nanomaterials, despite exceptional stability and biocompatibility, remain limited by high production costs.

Beyond material choice, successful translation requires design-for-regulation strategies integrated from early research stages:

- Selecting nanomaterials with existing ISO references, applying validated characterization protocols to ensure traceability, comparability, and regulatory alignment.
- Conducting preliminary risk assessments even in proof-of-concept studies can substantially accelerate downstream regulatory approval and reduce redesign cycles.
- Adopting simplified and scalable sensor architectures, favoring one-pot syntheses, self-assembly, and screen-printing over multistep functionalization routes to improve reproducibility and manufacturability.

The growing complexity of nanomaterial-enabled electrochemical biosensors—arising from multivariate electrochemical responses, matrix effects, and multiplexed detection—increasingly demands computational approaches beyond traditional models. Artificial intelligence (AI) and machine learning (ML) are emerging as transformative tools that can address multiple translational bottlenecks:

- Signal processing and pattern recognition: ML algorithms (support vector machines, random forests, neural networks) can extract relevant features from complex voltammetric, impedimetric, or chronoamperometric datasets, enabling discrimination of overlapping signals and real-time correction for drift, fouling, and environmental fluctuations, thereby improving operational stability without frequent recalibration.
- Predictive modeling for sensor optimization: AI-driven approaches can accelerate nanomaterial design by predicting structure-performance relationships (e.g., nanoparticle size vs. electrochemical activity) from limited experimental datasets, reducing trial-and-error iterations and guiding rational selection of surface chemistries and electrode architectures.
- Quality control and batch validation: Convolutional neural networks and anomaly detection algorithms applied to microscopy images (TEM, SEM) and spectroscopic

data (Raman, XPS) can automate nanomaterial characterization, ensuring compliance with regulatory specifications and identifying out-of-specification batches with higher throughput and consistency than manual inspection.

- Clinical decision support: Integration of biosensor outputs with patient-specific metadata through ML models can enhance diagnostic accuracy, stratify risk, and enable personalized treatment recommendations—particularly valuable for continuous glucose monitoring, cardiac biomarker panels, and infectious disease point-of-care platforms.

However, the integration of AI/ML into regulated biosensor platforms introduces its own challenges: the need for transparent, interpretable algorithms (particularly for medical devices under MDR/IVDR), requirements for extensive validation datasets representative of clinical diversity, and potential software-as-a-medical-device (SaMD) regulatory pathways that add approval complexity. Early engagement with regulatory bodies and adherence to emerging standards (e.g., ISO/IEC TR 24028 on AI trustworthiness, FDA guidance on AI/ML-based software) will be essential.

Ultimately, the impact of nanomaterial-enabled biosensors will be measured not only by analytical performance metrics but by their successful translation into routine clinical, industrial, and environmental applications. This transition requires treating nanomaterials as critical quality attributes from conception, integrating design-for-regulation principles throughout development, and leveraging computational intelligence to manage the inherent complexity of advanced sensing platforms. Bridging innovation and regulation in this holistic manner—spanning material science, electrochemistry, data science, and regulatory strategy—defines the defining challenge and opportunity for electrochemical biosensing in the coming decade.

Funding: This research was financed by the European Union—NextGeneration EU through the Italian Ministry of University and Research under PRIN 2022 RESOLVE, 202233FTW8 CUP B53D23013360006.

Data Availability Statement: The original contributions presented in this study are included in the article. Further inquiries can be directed to the corresponding authors.

Conflicts of Interest: Authors Stefano Giordani, Anna Placci, Pierluigi Reschiglian, Barbara Roda, Valentina Marassi and Andrea Zattoni were employed by the company byFlow srl (40129 Bologna, Italy). The remaining authors declare that the research was conducted in the absence of any commercial or financial re-lationships that could be construed as a potential conflict of interest.

References

1. Ronkainen, N.J.; Brian Halsall, H.; Heineman, W.R. Electrochemical Biosensors. *Chem. Soc. Rev.* **2010**, *39*, 1747–1763. [CrossRef]
2. Hammond, J.L.; Formisano, N.; Estrela, P.; Carrara, S.; Tkac, J. Electrochemical Biosensors and Nanobiosensors. *Essays Biochem.* **2016**, *60*, 69–80. [CrossRef]
3. Pohanka, M.; Skládal, P. Electrochemical Biosensors—Principles and Applications. *J. Appl. Biomed.* **2008**, *6*, 57–64. [CrossRef]
4. Wang, K.; Lin, X.; Zhang, M.; Li, Y.; Luo, C.; Wu, J. Review of Electrochemical Biosensors for Food Safety Detection. *Biosensors* **2022**, *12*, 959. [CrossRef]
5. Wu, J.; Liu, H.; Chen, W.; Ma, B.; Ju, H. Device Integration of Electrochemical Biosensors. *Nat. Rev. Bioeng.* **2023**, *1*, 346–360. [CrossRef] [PubMed]
6. Abdulbari, H.A.; Basheer, E.A.M. Electrochemical Biosensors: Electrode Development, Materials, Design, and Fabrication. *ChemBioEng Rev.* **2017**, *4*, 92–105. [CrossRef]
7. Sumitha, M.S.; Xavier, T.S. Recent Advances in Electrochemical Biosensors—A Brief Review. *Hybrid Adv.* **2023**, *2*, 100023. [CrossRef]
8. Li, L.; Wang, T.; Zhong, Y.; Li, R.; Deng, W.; Xiao, X.; Xu, Y.; Zhang, J.; Hu, X.; Wang, Y. A Review of Nanomaterials for Biosensing Applications. *J. Mater. Chem. B* **2024**, *12*, 1168–1193. [CrossRef]
9. Sharma, M.; Mahajan, P.; Alsubaie, A.S.; Khanna, V.; Chahal, S.; Thakur, A.; Yadav, A.; Arya, A.; Singh, A.; Singh, G. Next-Generation Nanomaterials-Based Biosensors: Real-Time Biosensing Devices for Detecting Emerging Environmental Pollutants. *Mater. Today Sustain.* **2025**, *29*, 101068. [CrossRef]

10. Andronico, L.A.; Chen, L.; Mirasoli, M.; Guardigli, M.; Quintavalla, A.; Lombardo, M.; Trombini, C.; Chiu, D.T.; Roda, A. Thermochemiluminescent Semiconducting Polymer Dots as Sensitive Nanoprobes for Reagentless Immunoassay. *Nanoscale* **2018**, *10*, 14012–14021. [CrossRef] [PubMed]
11. Di Fusco, M.; Quintavalla, A.; Lombardo, M.; Guardigli, M.; Mirasoli, M.; Trombini, C.; Roda, A. Organically Modified Silica Nanoparticles Doped with New Acridine-1,2-Dioxetane Analogues as Thermochemiluminescence Reagentless Labels for Ultrasensitive Immunoassays. *Anal. Bioanal. Chem.* **2015**, *407*, 1567–1576. [CrossRef] [PubMed]
12. Roda, B.; Deo, S.K.; O'Connor, G.; Moraskie, M.; Giordani, S.; Marassi, V.; Roda, A.; Daunert, S. Shining Light on Biosensors: Chemiluminescence and Bioluminescence in Enabling Technologies. *TrAC Trends Anal. Chem.* **2024**, *180*, 117975. [CrossRef]
13. Cho, I.-H.; Kim, D.H.; Park, S. Electrochemical Biosensors: Perspective on Functional Nanomaterials for on-Site Analysis. *Biomater. Res.* **2020**, *24*, 6. [CrossRef] [PubMed]
14. Shellaiah, M. A Review on Biomedical, Biomolecular, and Environmental Monitoring Applications of Cysteamine Functionalized Nanomaterials. *Micromachines* **2025**, *16*, 1144. [CrossRef]
15. Crapnell, R.D.; Banks, C.E. Electroanalytical Overview: Screen-Printed Electrochemical Sensing Platforms. *ChemElectroChem* **2024**, *11*, e202400370. [CrossRef]
16. Pour, S.R.S.; Calabria, D.; Emamiamin, A.; Lazzarini, E.; Pace, A.; Guardigli, M.; Zangheri, M.; Mirasoli, M.; Pour, S.R.S.; Calabria, D.; et al. Electrochemical vs. Optical Biosensors for Point-of-Care Applications: A Critical Review. *Chemosensors* **2023**, *11*, 546. [CrossRef]
17. Kim, J.; Jeong, J.; Ko, S.H. Electrochemical Biosensors for Point-of-Care Testing. *Bio-Des. Manuf.* **2024**, *7*, 548–565. [CrossRef]
18. Gauglitz, G. Analytical Evaluation of Sensor Measurements. *Anal. Bioanal. Chem.* **2018**, *410*, 5–13. [CrossRef]
19. Pandey, P.; Datta, M.; Malhotra, B.D. Prospects of Nanomaterials in Biosensors. *Anal. Lett.* **2008**, *41*, 159–209. [CrossRef]
20. Holzinger, M.; Le Goff, A.; Cosnier, S. Nanomaterials for Biosensing Applications: A Review. *Front. Chem.* **2014**, *2*, 63. [CrossRef] [PubMed]
21. Hasanzadeh, M.; Shadjou, N.; de la Guardia, M. Iron and Iron-Oxide Magnetic Nanoparticles as Signal-Amplification Elements in Electrochemical Biosensing. *TrAC Trends Anal. Chem.* **2015**, *72*, 1–9. [CrossRef]
22. Khan, A.; DeVoe, E.; Andreescu, S. Carbon-Based Electrochemical Biosensors as Diagnostic Platforms for Connected Decentralized Healthcare. *Sens. Diagn.* **2023**, *2*, 529–558. [CrossRef]
23. Ozbey, S.; Keles, G.; Kurbanoglu, S. Innovations in Graphene-Based Electrochemical Biosensors in Healthcare Applications. *Microchim. Acta* **2025**, *192*, 290. [CrossRef]
24. Şak, B.; Sousa, H.B.A.; Prior, J.A.V.; Şak, B.; Sousa, H.B.A.; Prior, J.A.V. Carbon Nanomaterial-Based Electrochemical Biosensors for Alzheimer's Disease Biomarkers: Progress, Challenges, and Future Perspectives. *Biosensors* **2025**, *15*, 684. [CrossRef]
25. Silveira, C.M.; Baur, J.; Holzinger, M.; Moura, J.J.G.; Cosnier, S.; Almeida, M.G. Enhanced Direct Electron Transfer of a Multihemic Nitrite Reductase on Single-Walled Carbon Nanotube Modified Electrodes. *Electroanalysis* **2010**, *22*, 2973–2978. [CrossRef]
26. Silveira, C.M.; Gomes, S.P.; Araújo, A.N.; Montenegro, M.C.B.S.M.; Todorovic, S.; Viana, A.S.; Silva, R.J.C.; Moura, J.J.G.; Almeida, M.G. An Efficient Non-Mediated Amperometric Biosensor for Nitrite Determination. *Biosens. Bioelectron.* **2010**, *25*, 2026–2032. [CrossRef] [PubMed]
27. Xiao, Y.; Patolsky, F.; Katz, E.; Hainfeld, J.F.; Willner, I. "Plugging into Enzymes": Nanowiring of Redox Enzymes by a Gold Nanoparticle. *Science* **2003**, *299*, 1877–1881. [CrossRef] [PubMed]
28. Patolsky, F.; Weizmann, Y.; Willner, I. Long-Range Electrical Contacting of Redox Enzymes by SWCNT Connectors. *Angew. Chem. Int. Ed.* **2004**, *43*, 2113–2117. [CrossRef]
29. Besteman, K.; Lee, J.-O.; Wiertz, F.G.M.; Heering, H.A.; Dekker, C. Enzyme-Coated Carbon Nanotubes as Single-Molecule Biosensors. *Nano Lett.* **2003**, *3*, 727–730. [CrossRef]
30. Gazzato, L.; Frasconi, M. Carbon Nanotubes and Their Composites for Flexible Electrochemical Biosensors. *Anal. Sens.* **2025**, *5*, e202400038. [CrossRef]
31. Velický, M.; Bradley, D.F.; Cooper, A.J.; Hill, E.W.; Kinloch, I.A.; Mishchenko, A.; Novoselov, K.S.; Patten, H.V.; Toth, P.S.; Valota, A.T.; et al. Electron Transfer Kinetics on Mono- and Multilayer Graphene. *ACS Nano* **2014**, *8*, 10089–10100. [CrossRef]
32. Yang, W.; Ratinac, K.R.; Ringer, S.P.; Thordarson, P.; Gooding, J.J.; Braet, F. Carbon Nanomaterials in Biosensors: Should You Use Nanotubes or Graphene? *Angew. Chem. Int. Ed.* **2010**, *49*, 2114–2138. [CrossRef]
33. Bonaccorso, F.; Lombardo, A.; Hasan, T.; Sun, Z.; Colombo, L.; Ferrari, A.C. Production and Processing of Graphene and 2d Crystals. *Mater. Today* **2012**, *15*, 564–589. [CrossRef]
34. Guo, X. Surface Plasmon Resonance Based Biosensor Technique: A Review. *J. Biophotonics* **2012**, *5*, 483–501. [CrossRef]
35. Tang, X.; Bansaruntip, S.; Nakayama, N.; Yenilmez, E.; Chang, Y.; Wang, Q. Carbon Nanotube DNA Sensor and Sensing Mechanism. *Nano Lett.* **2006**, *6*, 1632–1636. [CrossRef]
36. Li, C.; Curreli, M.; Lin, H.; Lei, B.; Ishikawa, F.N.; Datar, R.; Cote, R.J.; Thompson, M.E.; Zhou, C. Complementary Detection of Prostate-Specific Antigen Using In2O3 Nanowires and Carbon Nanotubes. *J. Am. Chem. Soc.* **2005**, *127*, 12484–12485. [CrossRef]
37. Gruner, G. Carbon Nanotube Transistors for Biosensing Applications. *Anal. Bioanal. Chem.* **2006**, *384*, 322–335. [CrossRef]

38. Shao, Y.; Wang, J.; Wu, H.; Liu, J.; Aksay, I.A.; Lin, Y. Graphene Based Electrochemical Sensors and Biosensors: A Review. *Electroanalysis* **2010**, *22*, 1027–1036. [CrossRef]
39. Kuila, T.; Bose, S.; Khanra, P.; Mishra, A.K.; Kim, N.H.; Lee, J.H. Recent Advances in Graphene-Based Biosensors. *Biosens. Bioelectron.* **2011**, *26*, 4637–4648. [CrossRef] [PubMed]
40. Li, Y.; Schluesener, H.J.; Xu, S. Gold Nanoparticle-Based Biosensors. *Gold Bull.* **2010**, *43*, 29–41. [CrossRef]
41. Xu, Q.; Mao, C.; Liu, N.-N.; Zhu, J.-J.; Sheng, J. Direct Electrochemistry of Horseradish Peroxidase Based on Biocompatible Carboxymethyl Chitosan–Gold Nanoparticle Nanocomposite. *Biosens. Bioelectron.* **2006**, *22*, 768–773. [CrossRef]
42. Mena, M.L.; Yáñez-Sedeño, P.; Pingarrón, J.M. A Comparison of Different Strategies for the Construction of Amperometric Enzyme Biosensors Using Gold Nanoparticle-Modified Electrodes. *Anal. Biochem.* **2005**, *336*, 20–27. [CrossRef]
43. Willner, B.; Katz, E.; Willner, I. Electrical Contacting of Redox Proteins by Nanotechnological Means. *Curr. Opin. Biotechnol.* **2006**, *17*, 589–596. [CrossRef] [PubMed]
44. Pingarrón, J.M.; Yáñez-Sedeño, P.; González-Cortés, A. Gold Nanoparticle-Based Electrochemical Biosensors. *Electrochim. Acta* **2008**, *53*, 5848–5866. [CrossRef]
45. Liu, Y.; Yang, Y.; Wang, G.; Wang, D.; Shao, P.-L.; Tang, J.; He, T.; Zheng, J.; Hu, R.; Liu, Y.; et al. Multiplexed Discrimination of SARS-CoV-2 Variants via Plasmonic-Enhanced Fluorescence in a Portable and Automated Device. *Nat. Biomed. Eng.* **2023**, *7*, 1636–1648. [CrossRef] [PubMed]
46. Li, Z.; Zhai, L.; Zhang, Q.; Zhai, W.; Li, P.; Chen, B.; Chen, C.; Yao, Y.; Ge, Y.; Yang, H.; et al. 1T′-Transition Metal Dichalcogenide Monolayers Stabilized on 4H-Au Nanowires for Ultrasensitive SERS Detection. *Nat. Mater.* **2024**, *23*, 1355–1362. [CrossRef]
47. Qaanei, M.; Taheri, R.A.; Eskandari, K. Electrochemical Aptasensor for Escherichia Coli O157:H7 Bacteria Detection Using a Nanocomposite of Reduced Graphene Oxide, Gold Nanoparticles and Polyvinyl Alcohol. *Anal. Methods* **2021**, *13*, 3101–3109. [CrossRef]
48. Brazaca, L.C.; Imamura, A.H.; Gomes, N.O.; Almeida, M.B.; Scheidt, D.T.; Raymundo-Pereira, P.A.; Oliveira, O.N.; Janegitz, B.C.; Machado, S.A.S.; Carrilho, E. Electrochemical Immunosensors Using Electrodeposited Gold Nanostructures for Detecting the S Proteins from SARS-CoV and SARS-CoV-2. *Anal. Bioanal. Chem.* **2022**, *414*, 5507–5517. [CrossRef]
49. Owino, J.H.O.; Arotiba, O.A.; Hendricks, N.; Songa, E.A.; Jahed, N.; Waryo, T.T.; Ngece, R.F.; Baker, P.G.L.; Iwuoha, E.I. Electrochemical Immunosensor Based on Polythionine/Gold Nanoparticles for the Determination of Aflatoxin B1. *Sensors* **2008**, *8*, 8262–8274. [CrossRef]
50. Amouzadeh Tabrizi, M.; Acedo, P. An Electrochemical Immunosensor for the Determination of Procalcitonin Using the Gold-Graphene Interdigitated Electrode. *Biosensors* **2022**, *12*, 771. [CrossRef]
51. Hemben, A.; Ashley, J.; Tothill, I.E. Development of an Immunosensor for PfHRP 2 as a Biomarker for Malaria Detection. *Biosensors* **2017**, *7*, 28. [CrossRef]
52. Labib, M.; Zamay, A.S.; Kolovskaya, O.S.; Reshetneva, I.T.; Zamay, G.S.; Kibbee, R.J.; Sattar, S.A.; Zamay, T.N.; Berezovski, M.V. Aptamer-Based Impedimetric Sensor for Bacterial Typing. *Anal. Chem.* **2012**, *84*, 8114–8117. [CrossRef]
53. Wang, S.; Cui, M.; Tang, H.; Zhang, M.; Zhang, Y. Gold Nanoparticles-Amplified Laccase-Based Electrochemical Biosensor Using Graphitized Carbon@boron Carbide as Electron Transfer Promoter. *Microchem. J.* **2024**, *207*, 111976. [CrossRef]
54. Gaba, S.; Jain, U. Electrochemical Immunosensor Based on Screen-Printed Electrodes Modified with Gold Nanoparticles for Highly Sensitive Detection of TGF-α. *Talanta Open* **2025**, *12*, 100590. [CrossRef]
55. Jaffrezic-Renault, N.; Martelet, C.; Chevolot, Y.; Cloarec, J.-P. Biosensors and Bio-Bar Code Assays Based on Biofunctionalized Magnetic Microbeads. *Sensors* **2007**, *7*, 589–614. [CrossRef]
56. Hsing, I.-M.; Xu, Y.; Zhao, W. Micro- and Nano- Magnetic Particles for Applications in Biosensing. *Electroanalysis* **2007**, *19*, 755–768. [CrossRef]
57. Stanciu, L.; Won, Y.-H.; Ganesana, M.; Andreescu, S. Magnetic Particle-Based Hybrid Platforms for Bioanalytical Sensors. *Sensors* **2009**, *9*, 2976–2999. [CrossRef] [PubMed]
58. Yang, L.; Ren, X.; Tang, F.; Zhang, L. A Practical Glucose Biosensor Based on Fe3O4 Nanoparticles and Chitosan/Nafion Composite Film. *Biosens. Bioelectron.* **2009**, *25*, 889–895. [CrossRef]
59. Zhuo, Y.; Yuan, P.-X.; Yuan, R.; Chai, Y.-Q.; Hong, C.-L. Bienzyme Functionalized Three-Layer Composite Magnetic Nanoparticles for Electrochemical Immunosensors. *Biomaterials* **2009**, *30*, 2284–2290. [CrossRef] [PubMed]
60. Cui, J.; Dong, N.; Wang, M.; Jiang, Y.; Miao, P. Porous Magnetic Nanoparticles-Based Electrochemical Biosensor for Determination of Mercury in the Aquatic Environment. *Part. Syst. Charact.* **2020**, *37*, 2000074. [CrossRef]
61. Zumpano, R.; Manghisi, M.; Polli, F.; D'Agostino, C.; Ietto, F.; Favero, G.; Mazzei, F. Label-Free Magnetic Nanoparticles-Based Electrochemical Immunosensor for Atrazine Detection. *Anal. Bioanal. Chem.* **2022**, *414*, 2055–2064. [CrossRef]
62. Boubezari, I.; Bessueille, F.; Bonhomme, A.; Raimondi, G.; Zazoua, A.; Errachid, A.; Jaffrezic-Renault, N.; Boubezari, I.; Bessueille, F.; Bonhomme, A.; et al. Laccase-Based Biosensor Encapsulated in a Galactomannan-Chitosan Composite for the Evaluation of Phenolic Compounds. *Biosensors* **2020**, *10*, 70. [CrossRef]

63. Hanoglu, S.B.; Man, E.; Harmanci, D.; Ruzgar, S.T.; Sanli, S.; Keles, N.A.; Ayden, A.; Tuna, B.G.; Duzgun, O.; Ozkan, O.F.; et al. Magnetic Nanoparticle-Based Electrochemical Sensing Platform Using Ferrocene-Labelled Peptide Nucleic Acid for the Early Diagnosis of Colorectal Cancer. *Biosensors* **2022**, *12*, 736. [CrossRef]
64. Singampalli, K.L.; Neal-Harris, C.; Yee, C.; Lin, J.S.; Lillehoj, P.B. Highly Reusable Electrochemical Immunosensor for Ultrasensitive Protein Detection. *Adv. Sens. Res.* **2024**, *3*, 2400004. [CrossRef] [PubMed]
65. Obeid, P.J.; Sari-Chmayssem, N.; Yammine, P.; Homsi, D.; El-Nakat, H.; Matar, Z.; Hamieh, S.; Koumeir, D.; Chmayssem, A. Designs and Materials of Electrodes for Electrochemical Sensors. *ChemElectroChem* **2025**, *12*, e202500230. [CrossRef]
66. *ISO/TR 13014:2012(En)*; Nanotechnologies—Guidance on Physico-Chemical Characterization of Engineered Nanoscale Materials for Toxicologic Assessment. ISO: Geneva, Switzerland, 2012. Available online: https://www.iso.org/obp/ui/en/#iso:std:iso:tr:13014:ed-1:v1:en (accessed on 17 October 2025).
67. *ISO 22412:2025(En)*; Particle Size Analysis—Dynamic Light Scattering (DLS). ISO: Geneva, Switzerland, 2025. Available online: https://www.iso.org/obp/ui/en/#iso:std:iso:22412:ed-3:v1:en (accessed on 17 October 2025).
68. *ISO 21363:2020(En)*; Nanotechnologies—Measurements of Particle Size and Shape Distributions by Transmission Electron Microscopy. ISO: Geneva, Switzerland, 2020. Available online: https://www.iso.org/obp/ui/en/#iso:std:iso:21363:ed-1:v1:en (accessed on 17 October 2025).
69. *ISO 17200:2020(En)*; Nanotechnologies—Nanoparticles in Powder Form—Characteristics and Measurements. ISO: Geneva, Switzerland, 2020. Available online: https://www.iso.org/obp/ui/en/#iso:std:iso:17200:ed-1:v1:en (accessed on 7 February 2026).
70. *ISO 17034:2016(En)*; General Requirements for the Competence of Reference Material Producers. ISO: Geneva, Switzerland, 2016. Available online: https://www.iso.org/obp/ui/en/#iso:std:iso:17034:ed-1:v1:en (accessed on 7 February 2026).
71. *ISO/TR 16197:2014(En)*; Nanotechnologies—Compilation and Description of Toxicological Screening Methods for Manufactured Nanomaterials. ISO: Geneva, Switzerland, 2014. Available online: https://www.iso.org/obp/ui/en/#iso:std:iso:tr:16197:ed-1:v1:en (accessed on 7 February 2026).
72. *ISO 10993-1:2018(En)*; Biological Evaluation of Medical Devices—Part 1: Evaluation and Testing Within a Risk Management Process. ISO: Geneva, Switzerland, 2018. Available online: https://www.iso.org/obp/ui/en/#iso:std:iso:10993:-1:ed-5:v1:en (accessed on 7 February 2026).
73. *ISO 10993-5:2009(En)*; Biological Evaluation of Medical Devices—Part 5: Tests for In Vitro Cytotoxicity. ISO: Geneva, Switzerland, 2009. Available online: https://www.iso.org/obp/ui/en/#iso:std:iso:10993:-5:ed-3:v1:en (accessed on 7 February 2026).
74. *ISO 10993-10:2021(En)*; Biological Evaluation of Medical Devices—Part 10: Tests for Irritation and Skin Sensitization. ISO: Geneva, Switzerland, 2021. Available online: https://www.iso.org/obp/ui/en/#iso:std:iso:10993:-10:ed-4:v1:en (accessed on 7 February 2026).
75. EFSA Scientific Committee. Guidance on risk assessment of nanomaterials to be applied in the food and feed chain: Human and animal health. *EFSA J.* **2018**, *16*, 5327. [CrossRef]
76. Implementation of the EFSA Scientific Committee guidance on nanomaterials in EFSA's scientific assessments. *EFSA Support. Publ.* **2021**, *18*, 6790E.
77. European Parliament and Council. Regulation (EU) 2017/745 on medical devices (Medical Device Regulation, MDR). *Off. J. Eur. Union* **2017**, *L 117*, 1–175.
78. European Parliament and Council. Regulation (EU) 2017/746 on in vitro diagnostic medical devices (In Vitro Diagnostic Regulation, IVDR). *Off. J. Eur. Union* **2017**, *L 117*, 176–332.
79. *ISO 13485:2016(En)*; Medical Devices—Quality Management Systems—Requirements for Regulatory Purposes. ISO: Geneva, Switzerland, 2016. Available online: https://www.iso.org/obp/ui/en/#iso:std:iso:13485:ed-3:v1:en (accessed on 7 February 2026).
80. *ISO 14971:2019(En)*; Medical Devices—Application of Risk Management to Medical Devices. ISO: Geneva, Switzerland, 2019. Available online: https://www.iso.org/obp/ui/en/#iso:std:iso:14971:ed-3:v1:en (accessed on 7 February 2026).
81. *ISO/IEC 17025:2017(En)*; General Requirements for the Competence of Testing and Calibration Laboratories. ISO: Geneva, Switzerland, 2017. Available online: https://www.iso.org/obp/ui/en/#iso:std:iso-iec:17025:ed-3:v1:en (accessed on 7 February 2026).